

# 2019 Masturi Effect of resin composition with Alumina ( $\text{Al}_2\text{O}_3$ ) and Silica ( $\text{SiO}_2$ ) on the X-Ray radiation absorbent dose at Lung-Phantom production

*by Masturi Masturi*

---

**Submission date:** 09-Sep-2020 02:56PM (UTC+0700)

**Submission ID:** 1382673995

**File name:** Susilo\_et\_al\_2019\_\_ICMSE2018.pdf (994.1K)

**Word count:** 3474

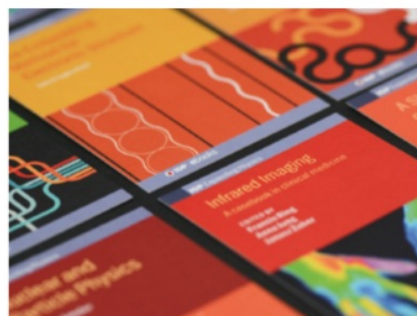
**Character count:** 17282

PAPER • OPEN ACCESS

3  
Effect of resin composition with Alumina ( $\text{Al}_2\text{O}_3$ ) and Silica ( $\text{SiO}_2$ ) on the X-Ray radiation absorbent dose at *Lung-Phantom* production

1  
To cite this article: Susilo *et al* 2019 *J. Phys.: Conf. Ser.* **1321** 032112

View the [article online](#) for updates and enhancements.



**IOP ebooks™**

Bringing together innovative digital publishing with leading authors from the global scientific community.

Start exploring the collection—download the first chapter of every title for free.

## Effect of resin composition with Alumina ( $\text{Al}_2\text{O}_3$ ) and Silica ( $\text{SiO}_2$ ) on the X-Ray radiation absorbent dose at Lung-Phantom production

Susilo<sup>1</sup>, Masturi<sup>1\*</sup>, W Hardyanto<sup>1</sup>, Mosik<sup>1</sup>, L Handayani<sup>1</sup>, S Santoso<sup>1</sup> and R Setiawan<sup>2</sup>

<sup>1</sup>Physics Department, Faculty of Mathematics and Natural Sciences, Universitas Negeri Semarang, Indonesia

<sup>2</sup>STIKES An-Nasher Kaliwadas, Sumber, Cirebon, West Java Indonesia

\*Corresponding author: masturi@mail.unnes.ac.id

**Abstract.** The ability of X-ray energy in the world of health is very useful to diagnose human organ, particularly the lung. The human lung is a very complex organ so the examination takes certain techniques to minimize the effects of radiation exposure. A lung phantom made from resin composition with alumina ( $\text{Al}_2\text{O}_3$ ) and silica ( $\text{SiO}_2$ ) was developed to eliminate negative effect of radiation. The purpose of this research is to find the closest value of density ( $D$ ) and coefficient of attenuation ( $\mu$ ) from the composition to be used as another alternative lung phantom. The lung phantom was made by different thickness of each composition of stepwedge. The method used was comparing between the density ( $D$ ) and attenuation coefficient ( $\mu$ ) of the sample and the lungs as a reference. The results were analysed using MATLAB 2015a Application with ROI grayscale reading. It was concluded that the composition of optimum lung phantom produced which is closed to reference value is 50% resin- $\text{Al}_2\text{O}_3$  content with density ( $D$ ) of 0.16, and 50% Resin -  $\text{SiO}_2$  composition with density ( $D$ ) of 0.18.

### 1. Introduction

Human organ is very complex and vital so the operation requires a certain technique [1]. The lung organ consists of tissues that are very soft, flat and plated, ie squamosa epithelial tissue that forms the pleura. Lung tissue can be categorized as a soft tissue that has a low density and atomic number so it needs an effective radiographic technique to produce a good image [2].

Factors affecting the intensity value of X-rays that expose an object are the difference of linear absorption coefficient and the difference of object thickness [3]. Epithelial and squamous tissues are soft tissues having similar linear absorption coefficients, so, theoretically, their radiographic contrast value is low. In order to obtain a good image, a soft tissue exposure technique requires the low tube voltage values (kV). Therefore, the determination of the soft tissue exposure factor needs to be optimized [4].

The results of exposure to X-ray radiation is very harmful to the body because X-rays have ionization power and great penetrating power. Therefore, phantom is very important to be used for learning in X-rays exposure in order to protect human from a direct experiment.

There are at least two reasons of using phantom. Firstly, the factory manufactured phantom is quite expensive. Its production requires a legal permission letter from the medical ethics commission.



Content from this work may be used under the terms of the Creative Commons Attribution 3.0 licence. Any further distribution of this work must maintain attribution to the author(s) and the title of the work, journal citation and DOI.

Another reason is a limited stock of a special sample for unusual disorder tissue needed for a particular research.

In a previous study, found that the phantom of the femur bone made of PVC material is less than ideal for displaying bone parts when exposed to X-rays. In addition, the material cannot be used to make another organ phantom. Based on these results, it can be said that the phantom made from PVC has not been feasible to be an alternative phantom [5]. Then, design phantom made using epoxy resin and alumina powder. Phantom designed by Wydra produced a good image of bone phantom during X-ray testing, but Wydra has not developed [6]. soft tissue substitute phantom in a form of stepwedge made from resin [4]. The developed soft tissue phantom was the one of thin thyroid tissue. By using this phantom, the digital image produced after X-rays exposure showed a good result with contrast and density value which was almost same with that of the real organ. But, this research was almost identical to that done by Serli, which was only done by making a difference between the epoxy and resin composition and has not used other materials such as silica or alumina to find which materials are best to be used as an alternative phantom.

Based on the above reasons, an alternative lung phantom using materials which have a relatively same characteristics with those of the tissue and human lung organ exposed by the X-rays was manufactured. In order to test the extent of eligibility of this artificial phantom, the phantom must have the same attenuation coefficient ( $\mu$ ) with the human lung organ. In addition to review the coefficient of attenuation ( $\mu$ ) of the phantom, relationship coefficient of attenuation ( $\mu$ ) phantom with its constituent material was defined in this research. This artificial phantom is expected to be able to replace factory-manufactured phantom at a more affordable price.

The alternative lung phantom made of alumina ( $\text{Al}_2\text{O}_3$ ) and silica, as the filler, epoxy resin and polyester resin as the polymer has been made in this research. The phantom has been made with a mixed variation of alumina ( $\text{Al}_2\text{O}_3$ ) and silica combined with epoxy resin and polyester resin, which was printed at the same thickness. Samples that have been made were irradiated using X-rays. This irradiation produced different contrasting radiographs depending on the sample compiler. The resulted radiograph was, then, measured by optical density using a densitometer measuring instrument, and the calculation was done to obtain the coefficient of attenuation ( $\mu$ ) of lung phantom and analyse the coefficient of absorption relationship to the size of the constituent particles. The result of radiograph will then be measured by the radiographic density using MATLAB software, and then the calculation will be performed to obtain the attenuation coefficient ( $\mu$ ) lung phantom and analysis of the relationship between the absorption coefficient and the size of the constituent particles.

## 2. Methods

Equipments used in this research included: X-ray, turren milling machine, magnetic stirrer, and scales. The materials used were epoxy resin and hardener,  $\text{Al}_2\text{O}_3$ , and  $\text{SiO}_2$ .

**Table 1.** Fraction of Resin- $\text{Al}_2\text{O}_3$  and Resin- $\text{SiO}_2$

Name of <i>Stepwedge</i>	Epoxy		$\text{Al}_2\text{O}_3/\text{SiO}_2$ (g)	Fraction (%)
	Resin (g)	Hardener (g)		
1	24.04	24.17	4.82	10%
2	22.07	22.05	8.82	20%
3	22.09	22.00	13.2	30%
4	22.19	22.01	17.6	40%
5	22.03	22.02	22.0	50%

The concentration between the polymer and the material for making the stepwedge is shown in Table 1, namely the difference in concentration between the resin and the  $\text{Al}_2\text{O}_3$  -  $\text{SiO}_2$  material. The difference in concentration between stepwedge one to the other must be different from certain multiples so that the results of the research are linear lines [4]. In this study the data collection method carried out by the author is primary data. The author uses the primary data method by making samples made from  $\text{Al}_2\text{O}_3$  Resin and  $\text{SiO}_2$  Resin which are then formed with a Turren Milling tool to form a stepwedge. Preparation of Measuring Equipment includes X-ray aircraft, detectors, laptops, research measuring sheets and stationery.



**Figure 1.** Stepwedge of Resin-  $\text{Al}_2\text{O}_3$  and Resin-  $\text{SiO}_2$

The mold is in the form of a beam and is formed in the form of a stepwedge which has been made from  $\text{Al}_2\text{O}_3$  Resin and  $\text{SiO}_2$  Resin as shown in Figure 1.

Samples are exposed by X-ray machine based on Digital Radiography (RADIG), and the results are in the form of digital images that are immediately visible on a computer [3]. If using conventional or digital X-ray machine such as CR and DR, the contrast resolution produced is not as good as when using RADIG X-ray aircraft, because in RADIG the image processing is gradual so that contrast resolution is better [3]. Sample exposed was carried out using the FFD parameter (focus source) as far as 100 cm, voltage 45 kV & 55 kV, current 16 mA, and exposure time 0.2 s. After exposed, the results of the sample digital images were cropped and measured radiograph density values using the MATLAB 2013a application with readings of ROI value processing (Region of Interest) and grayscale values of X-ray intensity on each sample image.

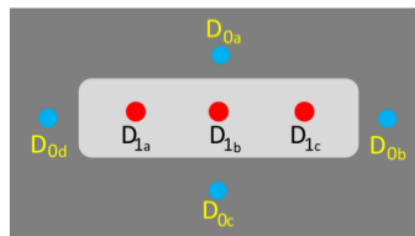


**Figure 2.** Radiograph density measurement point

Each sample image has three times reading the values at different points of each foreground shown as in Figure 2, this is intended to determine whether the sample that has been made homogeneous in

the density of the material. In addition to reading the radiograph density in the sample image, readings were also carried out at four points around the sample image. This reading is intended to read the radiographic density values in the background.

After obtained the density of radiograph, determining the attenuation coefficient value of each sample. the data is calculated according to the formula and in the form of tables to determine the level of accuracy.

### 3. Results and Discussion

The result of sample images was analysed by defining their intensity (I) using the Matlab based software. The X-ray intensity value can be found by changing the formula implementing GL (*gray level*) [4]

$$GL_x = GL_0 e^{-\mu x}$$

In order to obtain relationship between the transmittance and the thickness, the above equation can be changed as

$$\ln \frac{GL_0}{GL_x} = \mu x$$

$GL_0$  = gray level value in background,  $GL_x$  = gray level value on object,  $\mu$  = coefficient of linear attenuation ( $mm^{-1}$ ),  $x$  = material thickness (mm).

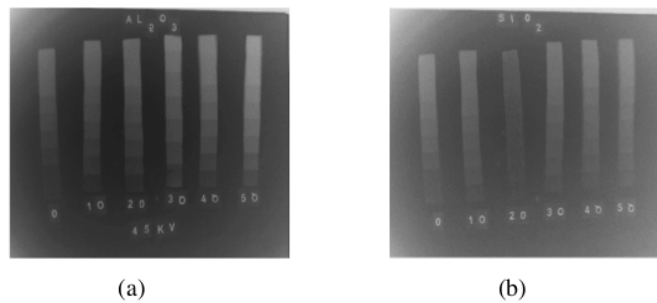


**Figure 3.** Digital image of Resin- $Al_2O_3$  (a) and Resin- $SiO_2$  (b) stepwedge at 45 kV

In addition to samples exposure using a 45-kV voltage, the samples were also exposed using 55 kV voltage with the same current, time and FFD values. Figure 3 shown the radiograph image of the Silica-resin-compiled sample appears to be more contrasted than the radiograph image of the alumina-resinous sample. Image contrast is a display of the ability of materials to absorb X-rays [7]. The ability of materials to absorb X-rays is based on their atomic number [8]. And X-ray absorption by a material also depends on the arrangement of the objects it passes, while the arrangement of objects depends on the atomic number, the smaller the atomic number, the smaller the absorption of X-rays [9]. Then Alumina which consists of an arrangement of elements  $Al_2$  and  $O_3$  and has an atomic number 13 has a smaller absorption power compared to Silica ( $SiO_2$ ) which has an atomic number of 14 in the same thickness state. Therefore, the composition of the sample consisting of Silica-resin has a clearer image contrast compared to the Alumina-resinous sample.



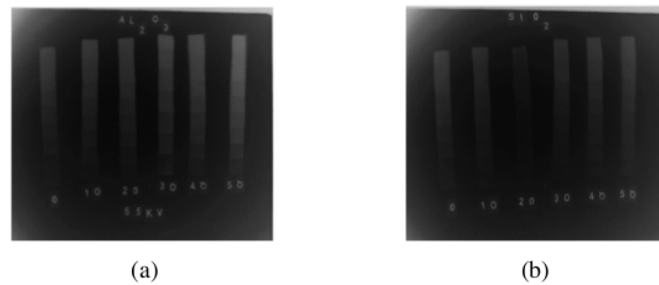


**Figure 4.** Digital image of Resin- $\text{Al}_2\text{O}_3$  (a) and Resin- $\text{SiO}_2$  (b) stepwedge at 55 kV

After being exposed to a tube voltage of 55 kV the sample image looks darker in the background as shown in Figure 4. The two images show a contrast difference using a different kV tube voltage. The above picture shows the contrast differences by using different kV tube voltages.

The contrast difference is caused by the tube voltage (kV) which affects the X-ray penetration [10]. This tube voltage was used to change the voltage used to accelerate the electrons in the tube [11]. The voltage of the tube (kV) is the control of the energy that produces X-rays. The voltage value of the tube (kV) determines the wavelength of the X-rays absorbed by a material.

$$\lambda = \frac{hc}{eV}$$

at the minimum wavelength, the equation changed be

$$\lambda \sim \frac{1}{V}$$

The shorter of X-ray wavelength (produced by higher kV), the higher energy of the X-rays. This leads the X-rays to be easy to penetrate the material [12].

The radiograph density is the result of variations in tube voltage differences. The density of the radiograph or optical density is the degree of blackish film density. A radiograph is said to be good when the contrast between the parts that make up the image can be clearly distinguished. The contrast of this radiograph is determined by the density of the film. If the contrast of radiographic results is better then the difference in density is greater [7].

Photographic density can be determined using equations [10]

$$D_0 = \text{Log} \left( \frac{I_0}{I_x} \right)$$

$D_0$  = density,  $I_0$  = rays intensity to the film,  $I_x$  = rays intensity to the object. The value of human lung density ranges from 0.25 to 2.5 [8]. Lungs organs including part of the thorax, the lung air GL value is smaller than 0,25. The calculation of the reference lung density (D), which is the lung of a hospital patient

**Table 2.** Lung density at 45 kV

Name	$I_0$	$\bar{I}_0$	$I_1$	$\bar{I}_1$	D
	65.71		37.04		
	63.58		40.20		
Lung	60.96	62.96	40.92	39.15	0.20
	61.44		39.54		
	63.11		38.06		

The data in Table 2 is the average density taken from 5 different intensity points.  $I_0$  is the initial intensity of X-rays that do not hit the object (background), while  $I_1$  is the intensity of the X-ray that hits the object (foreground). The lung is exposed to X-rays using 45 kV.

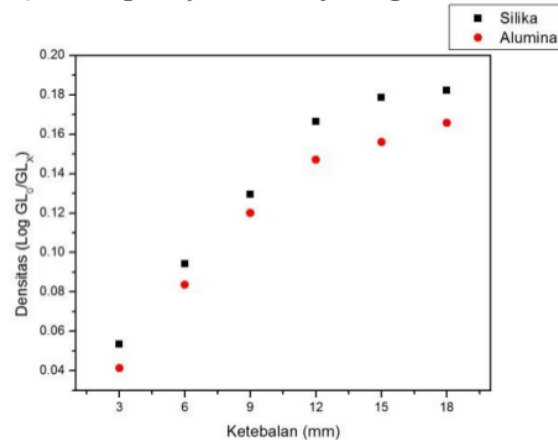


**Figure 5.** Relationship between density and thickness of stepwedge at 45 kV

Figure 5 shows the density value of Resin- $Al_2O_3$  and  $SiO_2$ . It can be seen that the closest density value (D) is a resin with 50%  $Al_2O_3$  and  $SiO_2$  content of 50% yielding density values of 0.16 and 0.18. This study found that the more  $Al_2O_3$  and  $SiO_2$  content, the value is closer to that of the lung density (D). The result of the difference in tube voltage not only affects optical density, but also the coefficient of attenuation. Contrast results from the difference in X-ray attenuation through an object [9].

The attenuation coefficient value ( $\mu$ ) of an object can be written in an equation that between  $I_x$  and  $I_0$  [13]

$$I_x = I_0 e^{-\mu x}$$

The above formula was changed to

$$\mu = \frac{1}{x} \left( \ln \frac{I_x}{I_0} \right)$$

**Table 3.** Coefficient attenuate of Lung at 45 kV

Name	$I_0$	$\bar{I}_0$	$I_1$	$\bar{I}_1$	$\mu$ mm <sup>-1</sup>
	65.71		37.04		
	63.58		40.20		
Lung	60.96	62.96	40.92	39.15	0.074
	61.44		39.54		
	63.11		38.06		

The coefficient of attenuation ( $\mu$ ) can also be defined as the ability of material to absorb an incoming radiation. If there is radiation coming on an object, then the value of intensity of the



radiation coming into the material and the intensity of radial out of the material will be different. This due to the attenuating nature of the material [14].

The data in Table 3 is the average density taken from 5 different intensity points.  $I_0$  is the initial intensity of X-rays that do not hit the object (background), while  $I_1$  is the intensity of the X-ray that hits the object (foreground). The lungs are exposed using 45 kV. Comparing the sample coefficient data with the coefficient of lung attenuation data as reference.

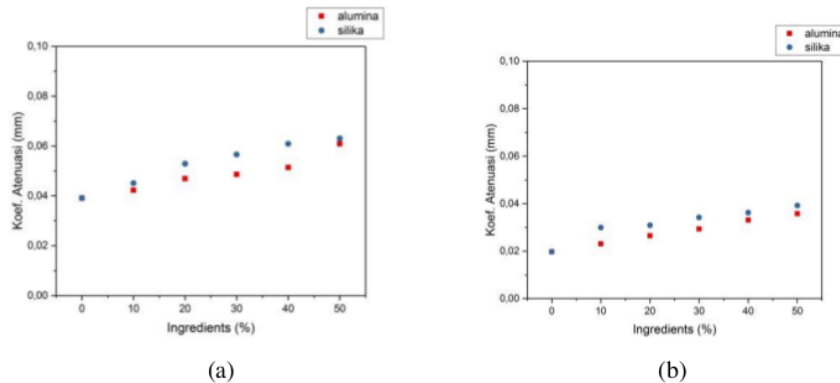


**Figure 6.** Coefficient attenuation graphic of 18 mm thickness at 45kV (a), and 55kV (b)

In Figure 6 shows graphs that increasing the attenuation coefficient value in the second material, both when exposed using a voltage of 45 kV or with a voltage of 55 kV. At 45 kV the attenuation coefficient value of the two materials is slightly different from the 55 kV graph which evaluates the graph of the attenuation coefficient value of the two materials whose values are almost entirely the same. In graph (a) the attenuation coefficient value of materials  $\text{Al}_2\text{O}_3$  and  $\text{SiO}_2$  is very different from graph (b) related to disturbances consisting of noise / noise in the image and unstable electricity voltage (up and down) when the sample material expands, but also displays the same graph namely coefficient value of material attenuation.

Based on the following graph shows that the greater the fraction of the mixture of materials, the greater the attenuation coefficient value of the material, the ability of X-rays to penetrate a material that increases the attenuation (thinning) to increase the value of the voltage kV tube [15].

The greater the voltage used, the stronger the ability of X-rays to penetrate the material needed for weakening material in adding X-rays. According to Suyatno and Bakhtiar (2011), the magnitude of the influence by materials depends on the following: (1) X-ray wavelengths, (2) arrangement of objects, (3) material density.

The greater the number of atoms of material, the greater the acquisition. The more atomic numbers increase, the better it emits x-rays that hit it [16]. In this study, it can be seen that samples of  $\text{SiO}_2$  resin resins have a greater absorption value because they have an atomic number of 14 compared to a mixed resin sample with  $\text{Al}_2\text{O}_3$  which has an atomic number of 13.

This study obtained more and more content of  $\text{Al}_2\text{O}_3$  and  $\text{SiO}_2$ , then obtained attenuation coefficient value ( $\mu$ ) lung. The coefficient attenuate ( $\mu$ ) composition of Resin- $\text{Al}_2\text{O}_3$  (red dot) and the composition of Resin- $\text{SiO}_2$  (blue dot), in Figure 6 shows that the value close to the reference is a resin containing 50%  $\text{Al}_2\text{O}_3$  and 50%  $\text{SiO}_2$  which produces a coefficient value attenuation of  $0.06 \text{ mm}^{-1}$  and  $0.07 \text{ mm}^{-1}$ . This study found that the more content of  $\text{Al}_2\text{O}_3$  and  $\text{SiO}_2$  approached the attenuation coefficient ( $\mu$ ) lung value.

The amount of X-rays absorbed by the material depends on the following: (1) X-ray wavelengths, (2) arrangement of objects, (3) thickness and (4) material density [17].

#### 4. Conclusion

Based on the analysis done in this research, it can be concluded that of density value (D) phantom which made as alternative phantom made of Resin -  $\text{Al}_2\text{O}_3$  is 0,16 with coefficient attenuation value ( $\mu$ )  $0,06 \text{ mm}^{-1}$ . Density (D) of Resin- $\text{SiO}_2$  is 0.18 with attenuation coefficient value ( $\mu$ )  $0.07 \text{ mm}^{-1}$ . The composition of the optimum phosphorus lung manufacture and its value close to the reference is 50% Resin-  $\text{Al}_2\text{O}_3$  and 50% Resin -  $\text{SiO}_2$ .

#### Acknowledgments

We would like to thank to the members of Physics Department, Universitas Negeri Semarang for their helpful discussion throughout the completion of this work.

#### References

- [1] Hsia C C W, Hyde D M and Weibel E R 2016 *Compr Physiol.* **6** 827
- [2] Kelly B 2012 *Ulst. Med. J.* **81**143
- [3] Susilo, Supriyadi, Sutikno, Sunarno and Setiawan R 2014 *JPF1* **8** 16
- [4] Sutrisno D A, Susilo and Masturi 2015 *Resin Based Stepwedge as A Substitute for Soft Tissue on Digital Radiographyc System* (ICMSE 2015, Semarang)
- [5] Moilanen P, Kilappa V, Nicholson P H F, Timonen J T and Cheng S 2004 *Ultrasound Med. Biol.* **30** 1517
- [6] Wydra and Adrian 2013 *Development of a New Forming Process to Fabricate a Wide Range of Fantoms that Highly Match the Acoustical Properties of Human Bone*. Electronic Theses and Dissertations Windsor, Ontario, Canada. Paper 4937.
- [7] Susilo, Maesadji T N, Kusminarto and Wahyu S B 2012 *J. Pendidikan Fisika Indonesia* **8** 98
- [8] Mukhtar A N and Sutanto H 2015 *Youngster Phys. J.* **4** 133
- [9] Suyatno F 2008 *Sem-Nas IV SDM Teknologi Nuklir Yogyakarta* **1** 503
- [10] Ningtias D R, Suryono S and Susilo 2016 *J. Pendidikan Fisika Indonesia* **12** 2355
- [11] Vassileva J 2014 *Br. J. Radiol.* **77** 648
- [12] Bartzsch S and Oelfke U 2017 *Phys Med Biol.* **62** 8600
- [13] Mousa A, Kusminarto K and Suparta G B 2017 *Res. India Publ.* **21** 0973
- [14] Akar A, Baltas H, Cevik U, Korkmaz F and Okumusoglu N T 2006 *J. Quant. Spectrosc. Radiat. Transf.* **102** 203
- [15] Tantra D A 2014 *Studi Pembuatan Perisai Radiasi Tembus Pandang dengan Paduan Timbal Acrylic sebagai Alternatif Pengganti Kaca Timbal*. Skripsi. Yogyakarta: Fakultas Teknik Universitas Gadjah Mada
- [16] Suyatno F 2008 *Sem-Nas IV SDM Teknologi Nuklir Yogyakarta* **1** 503
- [17] Raju D T and Shanth K 2014 *Int. J. Eng. Sci.* **3** 2319

# 2019 Masturi Effect of resin composition with Alumina (Al<sub>2</sub>O<sub>3</sub>) and Silica (SiO<sub>2</sub>) on the X-Ray radiation absorbent dose at Lung-Phantom production

## ORIGINALITY REPORT

7%

SIMILARITY INDEX

4%

INTERNET SOURCES

5%

PUBLICATIONS

4%

STUDENT PAPERS

## PRIMARY SOURCES

1

[eprints.whiterose.ac.uk](https://eprints.whiterose.ac.uk)

Internet Source

2%

2

A. F. Bouhdjar, M. Adaika, Am. Meftah, R. Boumaraf, Af. Meftah, N. Sengouga.

"Performance Study of the Micromorph Silicon Tandem Solar Cell Using Silvaco TCAD Simulator", Transactions on Electrical and Electronic Materials, 2019

Publication

2%

3

[pakar.unnes.ac.id](https://pakar.unnes.ac.id)

Internet Source

1%

4

Ian Yulianti, N. M. Dharma Putra, Budi Astuti, K. E. Kurniansyah, Z. A. F. Latif. "Fabrication and

characterization of polyester/polymethylmethacrylate buried waveguide for operation in visible light range", AIP Publishing, 2019

Publication

1%

5 Shengli Zhang, Lin Liao, Shuizhou Song, Changsuo Zhang. "Experimental and analytical study of the fibre distribution in SFRC: A comparison between image processing and the inductive test", Composite Structures, 2018  
Publication <1%

---

6 [icmseunnes.com](http://icmseunnes.com)  
Internet Source <1%

---

7 [shura.shu.ac.uk](http://shura.shu.ac.uk)  
Internet Source <1%

---

8 Submitted to The Manchester College  
Student Paper <1%

---

Exclude quotes On

Exclude matches < 4 words

Exclude bibliography On